

# A PROPOSAL FOR LASER SCANNERS SUB-PIXEL ACCURACY PEAK DETECTOR

J. Forest<sup>†</sup>, J.M. Teixidor<sup>†</sup>, J. Salvi<sup>†</sup> and E. Cabruja<sup>‡</sup>

<sup>†</sup>Universitat de Girona, Institut d'Informàtica i Aplicacions  
17003 Girona, Catalonia  
email: forest,qsalvi,jmteixi@eia.udg.es

<sup>‡</sup> Centre Nacional de Microelectrònica - CSIC  
08193 Cerdanyola del Vallès, Catalonia  
email: enric@cnm.es

## Abstract

*The demand for faster and more accurate three-dimensional digitisers is increasing dramatically in on-line production areas, while the more traditional application fields (i.e. inverse engineering or rapid prototyping) are increasingly incorporating non-contact scanners as their accuracy grows. Recently, the authors have published a short review on three dimensional laser scanners (Forest & Salvi 2002). An excellent source of information for diving into the active three dimensional computer vision world can be found in (Besl 1988).*

*This paper describes a numerical peak detector which performs at sub-pixel accuracy with very low computation, intended for use in three-dimensional laser scanners. Its performance in terms of detection error and computation time has been compared to other 4 numerical peak detection methods. This method has been optimised for fast computation in order to be included in a real-time vision architecture for fast range sensing.*

## 1 Introduction

The need for faster and more accurate three-dimensional laser scanners has been increasing since the first commercial such device was available. In addition, new companies devoted to the development of three-dimensional acquisition systems (either laser or light pattern projection), have flourished elsewhere. It is clear that the evolution of this field is subject to both the improvement of reconstruction accuracy and the increase of acquisition rates. The reconstruction accuracy depends on a set of cross-related issues like calibration, camera resolution, optics distortion, etc, while the range acquisition time is dependent on a clever image processing algorithm (responsible of segmenting the appropriate ROIs) in addition to a fast imaging sensor, capable of grabbing as many images per second as possible. In this paper, a numerical peak detector based on the computation of the zero-crossing of the peak first derivative is analysed. It uses a 2nd order filter for computing the first derivative, similarly to the estimator proposed by Blais and Rioux (Blais & Rioux 1986). As will be shown, the performance

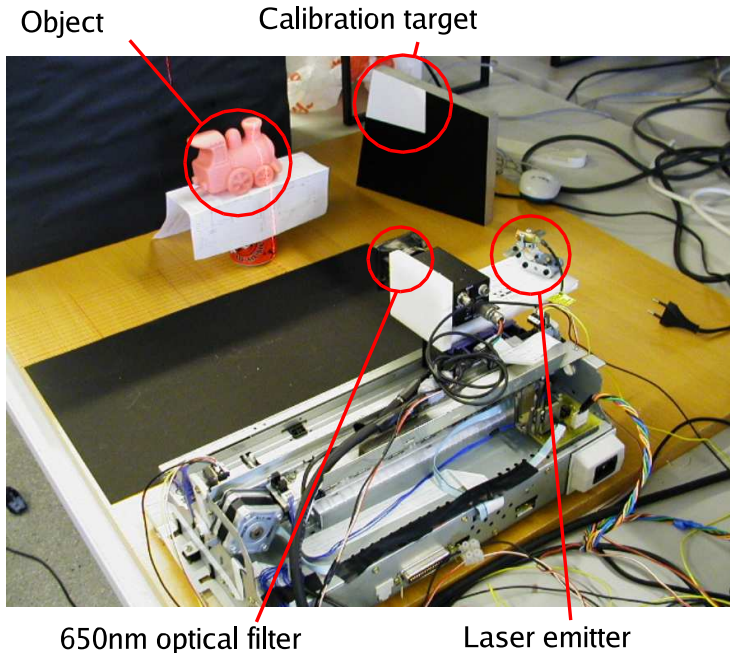


Figure 1: Overview of the scanner system.

in terms of peak location error of this method is similar to (Blais & Rioux 1986) when narrow peaks are considered, although it shows to be better when working with wider peaks. In addition, the computation time is lower. Trucco et. al. (Trucco et al. 1998) published an extensive, thorough work which included peak detector evaluations. The four methods used for comparison in this paper are the same as those compared in (Trucco et al. 1998).

Section 2 describes briefly the test-bench which has been used for digitising. The detection method is explained in section 3, while section 4 reports the experimental results of comparison with the other four estimators. The paper ends discussing conclusions and the further work which should be carried out.

## 2 Test-bench

Figure 1 shows the test-bench arranged for this experiment. The scanner consists of a solid state diode laser emitter of 1mW peak power ( $\lambda=650\text{nm}$ ) equipped with a cylindrical lens providing a light stripe at  $85^\circ$  aperture angle and 1.5mm in width at a 1m distance. In addition, a standard B/W camera (JAI CV-M50) with a  $1/2''$  752x582 pixels CCD sensor, together with a 16mm lens is included. A bandpass optical filter tuned with the laser wavelength has been used in order to better identify the stripe in the image, eliminating the need for software segmentation.

An ink jet printer mechanism has been used for scanning the scene both the camera and the laser emitter together. The system has been calibrated following Chen and Kak's (Chen & Kak 1987) algorithm.

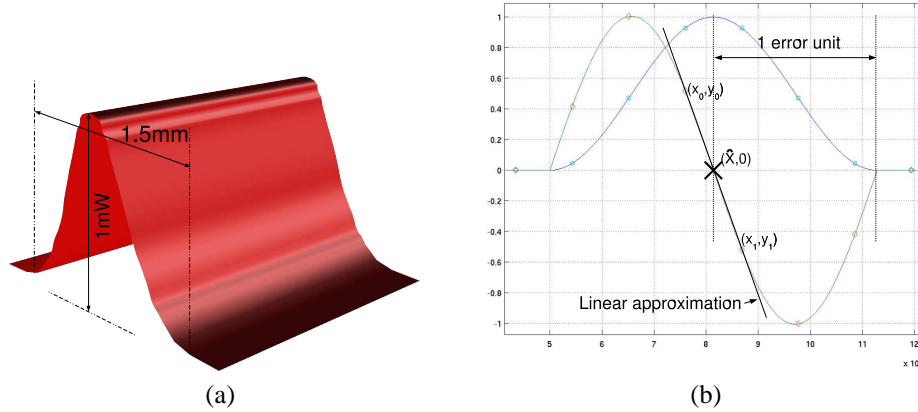


Figure 2: Laser Gaussian power profile (a) and Laser peak and first derivative (b).

### 3 Detection method

The laser stripe is generated using a solid state laser with a cylindrical lens which yields a Gaussian power profile, as shown in figure 2a. Considering a cross-section of the stripe and taking the first derivative in a noise-free experiment, the point at which the first derivative crosses the  $Y=0$  axis is the peak location (figure 2b). Hence, in order to get an accurate estimation, it seems to be reasonable if this zero-crossing point is computed. The problem with the peak determination is the discrete-nature of the CCD pixel array, which makes pixel to pixel interpolation necessary.

In this experiment, we have considered the first derivative to approach the shape of a sinusoidal pulse, hence applying the approximation  $\sin(x) \simeq x$  when  $x \simeq 0$ , it is likely that little error is committed. If we observe the sample points in the peak first derivative in figure 2b, and a line equation is interpolated between the two closest points to the  $Y=0$  axis in the sign change interval, the peak position can be estimated by computing the interpolated line zero-crossing. According to the notation in figure 2b, equation 1 shows how the peak position estimation ( $\hat{X}$ ) is computed. From equation 1 it is obvious that little computation must be performed in order to obtain  $\hat{X}$ . The first derivative has been approximated using a 2nd order filter, as shown in equation 2.

$$\hat{X} = x_0 - \frac{y_0 \cdot (x_1 - x_0)}{y_1 - y_0} \quad (1)$$

$$\dot{y}(i) = y(i+1) + y(i+2) - y(i-1) - y(i-2) \quad (2)$$

### 4 Comparison with other methods

The proposed peak detector has been compared with other four methods according to the formulae provided by (Trucco et al. 1998) and reproduced in table 1 for convenience. The term  $\hat{X}$  stands for the estimator value, while  $\delta$  is the decimal part which must be added to the integer peak guess. In table 1,  $i$  is the pixel guess (integer) for the peak position, while  $a$ ,  $b$  and  $c$  are the three maximum value pixels contained within

the peak width, with  $b$  being the maximum. For BR4,  $g(i)$  is the 2nd order filter value at the  $i$ -th pixel, while  $f(i)$  is the grey level value at the  $i$ -th pixel.

The four peak position estimators are the Blais and Rioux with 4th order filter (BR4), the Gaussian approximation (GA), Centre of mass (CM), and Linear interpolation (LI). In order to have a solid reference or *real* peak position, an ideal Gaussian profile has been synthesised using 62832 points in pulse width. As shown in figure 2b, the width of the Gaussian pulse has been normalised to  $\pm 1$  from the true peak position, hence the pulse resolution is of  $1/31416 = 3.1831 \cdot 10^{-5}$ .

In order to get a discrete pixel representation of the peak, different samplings have been performed, so 3,4,5,6,7 and 8 pixel width peaks have been obtained. In addition, Gaussian zero mean noise has been added to the samples varying the standard deviation from  $\sigma = 1/1000$  to  $\sigma = 1/3$ , which according to the unit amplitude of the pulse, it is equivalent to signal-to-noise ratios of 108.46dB to 8.48dB, respectively. The experiment has been performed so that for each value of  $\sigma$ , 100 different peak position estimates have been computed, obtaining their normalised distance to the real peak. Then, the average distance over the 100 estimates has been calculated. The average peak position errors have been depicted in figure 5, where discrete points show the average errors of the four compared methods while the continuous line show the average errors of the proposed estimator.

Considering a peak width of 3 to 5 pixels, the behaviour of the proposed estimator is very close to BR4, showing no significant differences with it. However, the peak estimator performance increases as the width of the peak increase, while BR4 shows bigger errors. The CM estimator yields big errors as the width of the peak increase, showing very low performance for more than 3 pixels. The highest performance is given by the GA estimator, regardless of the peak width, although logarithmic calculations are involved in the peak position estimation. Hence, either a high computation or different lookup tables are required. The LI estimator shows the poorest performance for more than 3 pixels, after CM. It is shown that for wide peaks, the proposed estimator is comparable to GA and shows better results for high noise levels, as can be observed for the cases of 7 and 8 pixels. All of the evaluated estimators but CM show acceptable stable results even for high noise levels ( $\sigma = 0.3$  or S/N=8.95dB).

Tables 2 and 3 show the mean and standard deviations of the charts in figure 5, for  $\sigma = 10^{-3}$  to  $\sigma = 0.3$ . As can be observed, the standard deviation and the mean of errors of the proposed estimator decreases as the pixel width increases, which can be observed in figure 5 as well, depicted as a 'smoother' and 'lower' curve. GA estimator shows a similar behaviour in  $\sigma$  only, while LI doesn't seem to be significantly affected by peak width. BR4 shows good performance in terms of both mean and  $\sigma$  for small peak width (4-6 pixels), but exhibits poorer results for more pixels.

In addition to the simulation results, a rough estimation of the real system has been performed, using a 4 to 5 pixel width stripe in both, the bi-dimensional case (see figures 6a and 6b), and the three-dimensional, regarding the Z direction only (see figures 7a and 7b).

## 5 Conclusions and Further work

A simple yet powerful method for the estimation of a laser stripe peak position with sub-pixel accuracy has been proposed. After a set of simulated experiments it has proved a high performance, especially for wider peaks. In addition, even at high noise levels it shows good results, while other methods start increasing the detection error at

Table 1: Estimator formulae according to Trucco

Estimator	Formula
GA	$\hat{X} = i - \frac{1}{2} \cdot \left( \frac{\ln(c) - \ln(a)}{\ln(a) + \ln(c) - 2 \cdot \ln(b)} \right)$
CM	$\hat{X} = i + \frac{c-a}{a+b+c}$
LI	$\hat{X} = \begin{cases} x - \frac{a-c}{2(b-a)} & c > a \\ x - \frac{a-c}{2(b-c)} & otherwise \end{cases}$
BR4	$\delta = \begin{cases} \frac{g(i)}{g(i)-g(i+1)} & f(i+1) > f(i-1) \\ \frac{g(i-1)}{g(i-1)-g(i)} & f(i+1) < f(i-1) \end{cases}$

Table 2: Means of normalised distances for  $\sigma = 10^{-3}$  to  $\sigma = 0.3$

Peak width	Prop.Est.	BR4	GA	CM	LI
3 pix.	0.0147	0.0149	0.0126	0.0130	0.0238
4 pix.	0.0062	0.0062	0.0047	0.0283	0.0098
5 pix.	0.0066	0.0067	0.0053	0.0468	0.0145
6 pix.	0.0067	0.0078	0.0057	0.0541	0.0151
7 pix.	0.0050	0.0091	0.0046	0.0484	0.0153
8 pix.	0.0044	0.0100	0.0043	0.0451	0.0152

Table 3: Std. dev. of normalised distances for  $\sigma = 10^{-3}$  to  $\sigma = 0.3$

Peak width	Prop.Est.	BR4	GA	CM	LI
3 pix.	0.0012	0.0012	0.0011	0.0011	0.0015
4 pix.	0.0006	0.0006	0.0005	0.0021	0.0007
5 pix.	0.0006	0.0006	0.0007	0.0029	0.0007
6 pix.	0.0004	0.0005	0.0006	0.0034	0.0008
7 pix.	0.0004	0.0009	0.0007	0.0030	0.0007
8 pix.	0.0005	0.0012	0.0009	0.0027	0.0009

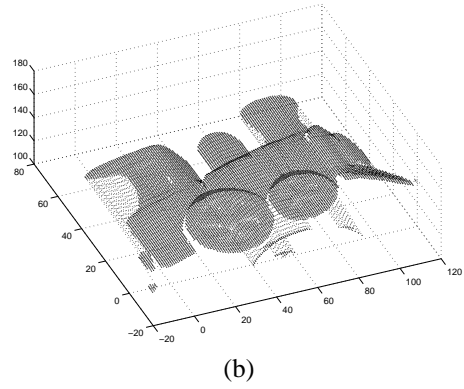
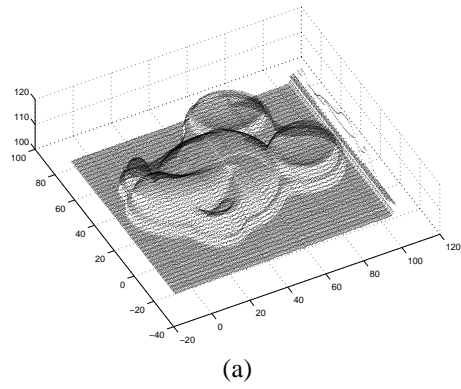


Figure 3: The most famous mouse in the world (a) and A little train locomotive (b).



Figure 4: Pictures of the real toys.

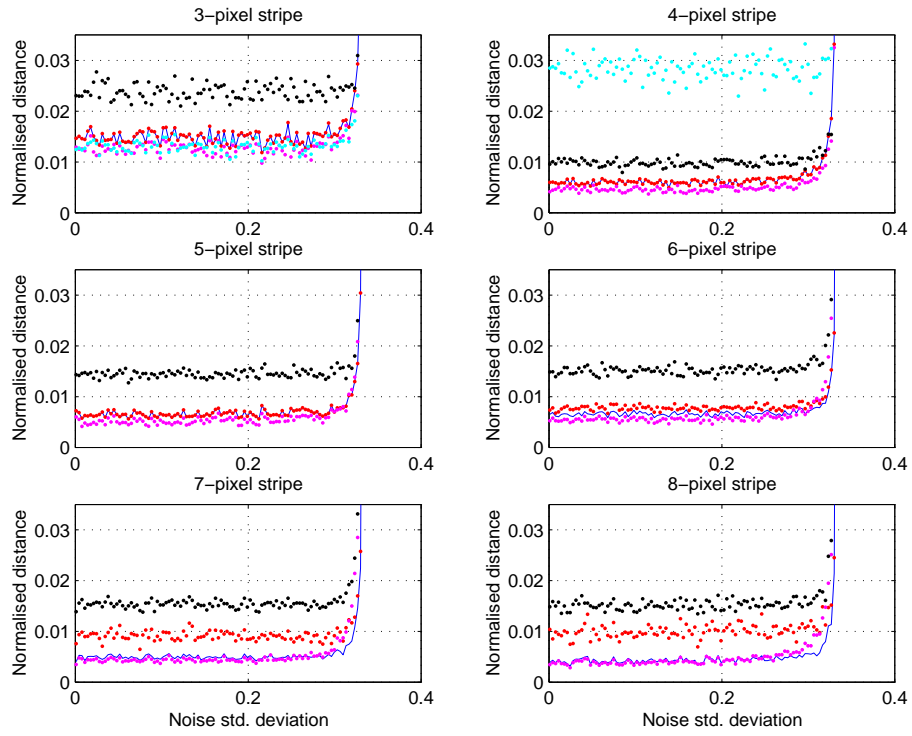


Figure 5: Average errors for the 5 evaluated methods.

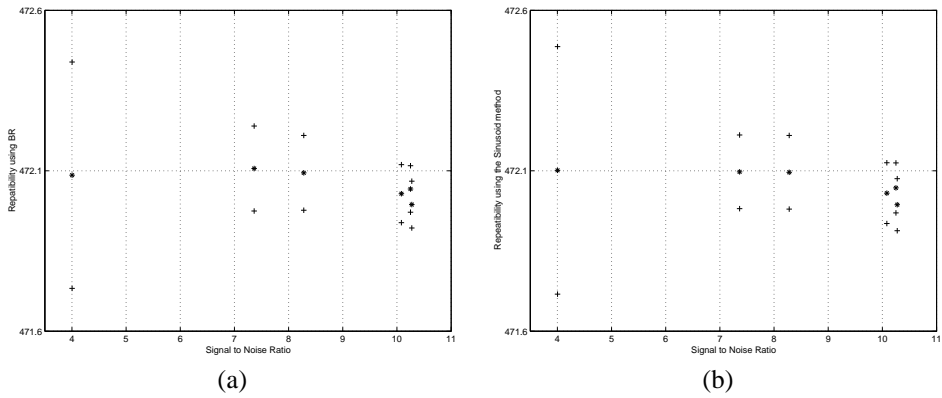


Figure 6: Repeatability of (a) BR method and (b) Sinusoid method versus S/N evaluated in pixels.

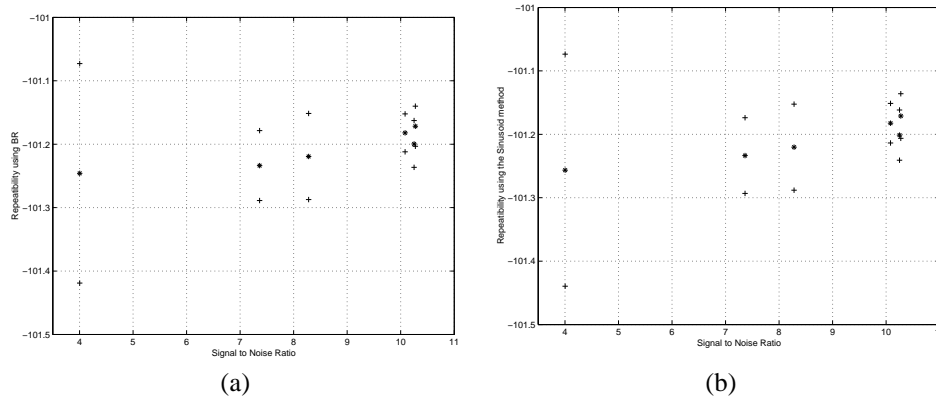


Figure 7: Repeatability of (a)BR method and (b)Sinusoid method versus S/N evaluated in mm in Z.

lower noise levels. This makes the proposed estimator to be usable for a wider noise range. The error measurements have been made considering a normalised synthesised peak waveform for easily compare with the other methods, and the results have been reported in normalised distance (that is in %) for avoiding the dependence on *pixel units*.

Although the experiments have been made in the bidimensional domain only, it is worth making error measurements in the three-dimensional domain in order to test completely its performance. This is going to be made in the next 1-2 months, when a suitable mechanical measuring bench will be available in our lab. However, figures 3a and 3b show how two toys have been digitised, showing visually acceptable results, while figure 4 show pictures of the real objects.

## References

- Besl, P. (1988). Active, optical range imaging sensors, *Machine Vision and Applications* **1**: 127–152.
- Blais, F. & Rioux, M. (1986). Real-time numerical peak detector, *Signal Processing*, Vol. 11, pp. 145–155.
- Chen, C. & Kak, A. (1987). Modeling and calibration of a structured light scanner for 3-d robot vision, *Proceedings of the IEEE conference on robotics and automation*, IEEE, pp. 807–815.
- Forest, J. & Salvi, J. (2002). A review of laser scanning three-dimensional digitisers, *Intelligent Robots and Systems, 2002*, IEEE/RSJ, pp. 73–78.
- Trucco, E., Fisher, R., Fitzgibbon, A. & Naidu, D. (1998). Calibration, data consistency and model acquisition with a 3-d laser striper, *International Journal of Computer Integrated Manufacturing* **11**(4): 292–310.